Title Spatial clustering of high load ocular *Chlamydia trachomatis* infection in trachoma: A cross-sectional population-based study

Authors Anna Last[1#], Sarah Burr[2], Neal Alexander[3], Emma Harding-Esch[1], Chrissy h. Roberts[1], Meno Nabicassa[4], Eunice Teixeira da Silva Cassama[4], David Mabey[1], Martin Holland[1], Robin Bailey[1]

[1]Clinical Research Department, London School of Hygiene and Tropical Medicine, Keppel Street, London, WC1E 7HT, United Kingdom

[2]Disease Control and Elimination Theme, Medical Research Council Unit The Gambia, P.O. Box 273 Banjul, Atlantic Boulevard, Fajara, The Gambia

[3]MRC Tropical Epidemiology Group, London School of Hygiene and Tropical Medicine, Keppel Street, London, WC1E 7HT, United Kingdom

[4]Programa Nacional de Saúde de Visão, Ministério de Saúde Publica, P.O. Box 50, Avenida de Unidade Africana, Bisssau, Guiné Bissau

[#]Corresponding Author: Clinical Research Department, London School of Hygiene and Tropical Medicine, Keppel Street, London WC1E 7HT. Telephone: +44 (0) 207 927 2566. Email: anna.last@lshtm.ac.uk

Abstract

Chlamydia trachomatis (Ct) is the commonest cause of bacterial sexually transmitted infection and infectious cause of blindness (trachoma) worldwide. Understanding the spatial distribution of *Ct* infection may enable us to identify populations at risk and improve our understanding of *Ct* transmission. In this study we sought to investigate the spatial distribution of *Ct* infection and the clinical features associated with high *Ct* load in trachoma-endemic communities on the Bijagós Archipelago (Guinea Bissau). We collected 1507 conjunctival samples and corresponding detailed clinical data during a cross-sectional population-based geospatially-representative trachoma survey. We used droplet digital PCR to estimate *Ct* load on conjunctival swabs. Geostatistical tools were used to investigate clustering of ocular *Ct* infections. Spatial clusters (independent of age and gender) of individuals with high *Ct* loads were identified using local

indicators of spatial association. We did not detect clustering of individuals with low load infections. These data suggest that infections with high bacterial load may be important in *Ct* transmission. These geospatial tools may be useful in the study of ocular *Ct* transmission dynamics and as part of trachoma surveillance post-treatment, to identify clusters of infection and thresholds of *Ct* load that may be important foci of re-emergent infection in communities.

INTRODUCTION

Chlamydia trachomatis is the leading infectious cause of blindness and the most common sexually transmitted bacterium. Trachoma is caused by infection with ocular strains of *C. trachomatis* and manifests as distinct clinical syndromes, beginning with an acute self-limiting kerato-conjunctivitis which may progress to chronic inflammatory disease with subsequent conjunctival scarring and blinding sequelae. A spectrum of disease severity exists, which can be graded objectively [1,2].

The World Health Organization (WHO) advocates the implementation of the SAFE strategy (Surgery for trichiasis, Antibiotics for active infection, Facial cleanliness to prevent disease transmission and Environmental improvement to increase access to water and sanitation) for trachoma elimination. Mass Drug Administration (MDA) of azithromycin aims to clear infection from communities such that trachoma ceases to be a public health concern [3].

Understanding the spatial distribution of disease and infection in trachoma-endemic regions is increasingly recognized in national trachoma control programme planning, enabling the identification of at risk populations and prioritization of target areas for control and implementation and optimal scaling of SAFE [4-8]. It may also be important in understanding transmission, transmission thresholds and the dynamics of spread and recovery from infection following intervention.

Spatial analysis provides powerful methods to study the relationship between active trachoma and ocular infection with *C. trachomatis*. The spatial relationship between disease and infection defined over space is termed spatial dependence. This is measured as the existence of statistical association (dependence) between disease and infection associated with location. To explore spatial dependence measures of spatial autocorrelation are used. Spatial autocorrelation assumes that near objects are more related than distant objects. In the context of infectious

diseases, this concept may be applied to explore the relationship between infection and disease where the spatial distribution can be used to define underlying processes such as exposure or transmission. Spatial regression models can thus be used to understand the epidemiology of active trachoma and *C. trachomatis* infection.

Global spatial autocorrelation statistics are used to describe the overall spatial patterns in the data. Local indicators of spatial association take actual values of observations in the context of adjacent values allowing mapping and definition of clusters at exact locations. This allows for the examination of small-scale heterogeneity and identification of statistically significant clusters and outliers of similar observations in space. In the context of global spatial patterns described above, this provides us with a greater understanding of the relationship between infection and disease.

In this study we applied molecular and geostatistical tools to investigate the spatial epidemiology of *C. trachomatis* infection and active trachoma in a population-based study conducted in a trachoma-hyperendemic treatment-naïve population from the Bijagós Archipelago of Guinea Bissau in West Africa. This is the first study to use local indicators of spatial association using individual-level *C. trachomatis* load data in the context of spatial dependence to investigate the relationship between infection and disease. This is important in understanding the epidemiology of ocular *C. trachomatis* infection and may inform further studies on *C. trachomatis* transmission dynamics, which are fundamental to successful trachoma elimination and surveillance strategies.

MATERIALS AND METHODS

Ethical Approval

This study was conducted in accordance with the declaration of Helsinki. Ethical approval was obtained from the Comitê Nacional de Ética e Saúde (Guinea Bissau), the LSHTM Ethics Committee (UK) and The Gambia Government/MRC Joint Ethics Committee (The Gambia). Written informed consent was obtained from all study participants or their guardians on their behalf if they were children. A signature or thumbprint is considered an appropriate record of consent in this setting by the above ethical bodies. After survey completion all

communities on the study islands were treated with a single height-based dose of oral azithromycin in accordance with WHO and national protocols.

Study Area

The Bijagós Archipelago has a total area of more than 10,000 km^2 and lies between N $11^0$38'19.68" and N $10^0$51'40.32", W $16^0$29'38.40" and W $15^0$27'17.28". The surface area covers approximately 900 km^2, of which 350 km^2 is mangrove forest [9]. Maximum altitude is 50m. The climate is humid and tropical, with a rainy season from May-November, when average monthly rainfall is 400mm^3 [10]. Mean monthly temperature is 27.3^{0}C (25.1-29.2^{0}C), with peak temperatures prior to the rainy season. There are 88 islands and islets of which approximately 20 are permanently inhabited. The remainder are inhabited periodically for seasonal agriculture and traditional initiation ceremonies. The study was conducted on four islands of the archipelago (*Figure 1*). These four islands comprise a total rural population of 5,613 (National Population Census, 2010, Instituto Nacional de Estatística, Guiné-Bissau) and a total area of 215km^2.

Study Design and Study Population

Trachoma survey methodology and this study population have been described previously [11,12-15]. To satisfy adequate geospatial representation at village-level, we included all 38 villages on the four study islands and randomly sampled one in five households (with a minimum of five per village) from each. All were sampled if there were fewer than six households in the village. Small villages are thus over-represented by the minimum sampling criteria imposed. Data were geo-coded at household and village level using the Garmin eTrex H handheld Global Positioning Systems (GPS) unit (Garmin Ltd., UK).

Clinical Examination and Conjunctival Sampling

A single validated examiner assessed each participant using the WHO simplified and modified FPC grading systems [1,2]. In the modified FPC system, follicles (F), papillae (P) and conjunctival scarring (C) are each assigned a separate grade from 0-3. FPC grades of F2/3 or P3 equate to a diagnosis of active trachoma (TF (follicular trachoma) or TI (inflammatory trachoma) by the WHO simplified system) and a grade of C2/3 (and in some cases C1) equates to a diagnosis of TS (trachomatous scarring). A trachoma grade was assigned to the upper tarsal

conjunctivae of each consenting participant using adequate light and a 2.5x binocular magnifying loupe. Both methods were used in order that study data should be comparable to data used by trachoma control programmes and research studies requiring detailed information related to disease severity and have been used previously in similar settings [16,17].

Samples were taken from the left upper tarsal conjunctiva of each participant with Dacron swabs (Fisher Scientific, UK) using a well-tolerated standardized procedure described in previous studies [11,12,13,18,19].

Detection and Quantitation of *C. trachomatis* ocular infection

DNA extraction and droplet digital PCR (ddPCR) (Bio-Rad Laboratories, Hemel Hempstead, UK) were conducted as described previously [11-13]. We used *C. trachomatis* plasmid-based ddPCR to diagnose infection and a single-copy pathogen chromosomal gene (*omcB*) to estimate pathogen load in each plasmid-positive sample [12,13]. The plasmid-based screening PCR included primers for human DNA (RPP30). A sample was deemed adequate if sufficient quantities of RPP30 DNA were present on PCR as defined previously [12,13].

Estimated quantities of *omcB* (*C. trachomatis* load) and plasmid are expressed as copies/swab. This is a method that we have previously employed for similar analyses [11,16,20-23]. Data reported by Solomon *et al.* (showing a clear reduction in *C. trachomatis* load and disease severity in a trachoma-endemic community in Tanzania following mass drug treatment with azithromycin (MDA) [24]), and Alexander *et al.* (showing a reduction in community *C. trachomatis* load (calculated using the same method) following MDA [25]), provide evidence that measuring *C. trachomatis* load as copies/swab in this context is appropriate. We do not report *C. trachomatis* load per eukaryotic cell since inflammatory cells are attracted to the conjunctiva in the presence of ocular *C. trachomatis* infection which would be included amongst sampled cells and may artefactually decrease the *C. trachomatis* load. This is of particular concern in active trachoma, where inflammation can be intense and result in high loads of human cellular material on a swab. This phenomenon has also been noted in urogenital *C. trachomatis* infection [26].

Statistical Analysis

C. trachomatis quantitation data were processed as described previously [12,13]. GPS data were downloaded into MapSource v16.16.3 (Garmin Ltd., UK). All data were double entered into a customised database (Microsoft Access 2007) and discrepancies resolved through reference to source documents. Data were cleaned and analysed in STATA 13 (Stata Corporation, College Station, Texas USA). Statistical significance was determined at the 5% level.

Mixed effects linear regression models of C. trachomatis load and Clinical Phenotype

C. trachomatis load data were log(e) transformed where indicated. The geometric mean of load, respective standard error (SE) and 95% confidence intervals (CI) were calculated. An analysis of variance (ANOVA) with pair-wise comparisons was used to compare load across detailed clinical phenotypes. Assessment of group differences and multiple comparisons were adjusted for using the Scheffé correction [27]. Associations between load and detailed clinical phenotype were examined using univariable and multivariable mixed effects linear and logistic regression models accounting for household-level clustering detected in previous studies [11].

Geostatistical Analyses

Geocoded data were projected into UTM Zone 28N. ArcGIS 10.1 (ESRI Inc., USA) and the R statistical package v3.0.2 (The R Foundation for Statistical Computing, http://www.r-project.org using spdep, automap and nlme packages) were used for all geostatistical analyses [28-30]. In the following analyses, the zone of indifference is used to define adjacency. This method assumes that each observation has local influence that decreases with distance beyond a critical distance cut-off, resulting in an adapted model of impedance, or distance decay, such that all features have an impact on all other features, but this impact decreases with distance. The crucial cut-off used in this study is derived from the distance over which spatial autocorrelation occurs in these data and relates to the village boundaries, assuming impedance as described above. Previously we have shown that clustering exists at this level in these communities [11], which supports using this threshold. This method is appropriate for point data and takes into account the extent of spatial autocorrelation in selecting data-driven threshold cut-offs [31].

Spatial Autocorrelation

The Moran's I statistic was used to evaluate global spatial autocorrelation in the distribution of the household-level prevalence of disease and infection. The values of Moran's I range between -1 and +1. A value close to -1 indicates negative autocorrelation (complete dispersion) whilst a value close to +1 indicates positive autocorrelation (clustering) of features. A value close to 0 suggests random arrangement. Z-scores and p-values are assigned to ascertain whether spatial autocorrelation is statistically significant [32]. Since the Moran's I statistic can be sensitive to skewed distributions, a permutation test was used to verify the results. This uses Monte Carlo simulations to generate a Moran's I sampling distribution [33].

Empirical semivariograms were used to obtain the distance range over which spatial autocorrelation occurs using the average squared distance between paired data values against the distance (or lag) separating the pairs to estimate the spatial covariance structure of the data to inform the geostatistical models [34].

Linear and logistic mixed effects regression models were also applied to examine the effect of spatial autocorrelation on clustering. We used the covariance structure to compare models with and without a spatial component. The log likelihood, Akaike information criterion (AIC) and Bayesian information criterion (BIC) were used to compare models [35].

Local Indicators of Spatial Association: Cluster-Outlier Analyses

Clustering and outlier analysis was applied using the local (Anselin) Moran's I statistic in ArcGIS 10.1 Spatial Statistics Toolbox (ESRI Inc., USA). The zone of indifference was used to define adjacency and the Euclidean distance threshold was derived from empirical semivariograms as described above. The Euclidean distance threshold was thus the distance over which the highest positive spatial autocorrelation for *Ct* infection existed. Together these account for the geography (islands with populated (villages) and non-populated areas) [36]. Individuals' *Ct* loads were used as the variable of interest. Since these populations and areas are small with little ecological variation, this single threshold value is sufficient. A positive value for I indicates that a feature has adjacent features with similarly high or low attributable values (a cluster). A negative value for I indicates that adjacent features have dissimilar values and that this feature is an outlier. Cluster-Outlier analysis identifies spatial clusters of features with high or low values and spatial outliers by calculating Moran's I, Z-scores, p-values and a code to represent the cluster type. Cluster types are defined as clusters of high values (HH, High-High), clusters of low

values (defined as above) (LL, Low-Low), a high value outlier surrounded by predominantly low values (HL, High-Low) and a low value outlier surrounded by predominantly high values (LH, Low-High). A group of geospatially proximal infections where the bacterial load values are not statistically similar is defined as a non-significant cluster.

In this analysis 'low' values include both low values related to low load infections and null (zero) values related to uninfected individuals. To explore this, these analyses were conducted first on the whole data set, including uninfected individuals with a 'zero' value for infectious load, and then on infected individuals only.

RESULTS

Trachoma and *C. trachomatis* infection prevalence is hyperendemic in this population and is described elsewhere in detail [11-13]. All swab samples in the study were positive for the presence of the human DNA target RPP30. *C. trachomatis* load was skewed, with the majority of cases having low copy numbers (<1000 copies/swab). Log-(e) transformation removed the skew (skewness -0.106, *p=0.5454*) in these analyses.

C. trachomatis bacterial load and clinical disease severity in individuals with *C. trachomatis* infection

The geometric mean of estimated *omcB* copies/swab present in clinically normal conjunctivae (F0/P0/C0) was 294 copies/swab (95% C.I. 165-524). In clinically active trachoma it was 8562 copies/swab (95% C.I. 5412-13546). Significantly higher loads were detected in individuals with increasing F and P scores (*Table 1*). *C. trachomatis* load by age and clinical phenotype is shown in *Figure 2*. The majority of infections with high loads were in children under 10 years of age with active trachoma.

Spatial structure of active trachoma and *C. trachomatis* infection

Significant positive spatial autocorrelation was evident for *C. trachomatis* infection (Moran's I=0.19, *p<0.0001*) but not active trachoma (Moran's I=0.07, *p=0.0659*). Semi-variograms demonstrate that autocorrelation in infection is negligible in distances greater than

1719m (*Figure 3*). We found no evidence of spatial autocorrelation in the distribution of *C. trachomatis* load (Moran's I=0.05, *p=0.4464*).

C. trachomatis load was the strongest predictor of clinically active trachoma. In accordance with the semi-variograms, including spatial structure in multivariable mixed effects regression analyses for active trachoma and *C. trachomatis* infection improves the fit of the models (*Table 2*).

Inflammatory and follicle scores were strongly associated with bacterial load. Inclusion of the spatial structure in models predicting *C. trachomatis* load improved the fit, but the effect of spatial dependence becomes undetectable when age and disease severity scores are included, thus resolving residual spatial variation (*Table 3*).

Cluster and outlier analysis of *C. trachomatis* infection

High load infections were clustered with other high load infections (HH clusters) (*Figure 4*). Outliers where there was a single low load infection amidst predominantly high load infections (HL) were also demonstrated. There was no clustering of low load infections (or zero-values from uninfected individuals) (LL clusters) and there were no statistically significant outlying high loads surrounded by predominantly low loads (LH). Analyses were conducted on the whole data set and infections only as described above. There were no individuals with infections below 10,000 *omcB* copies/swab noted within a HH cluster or as a HL outlier.

DISCUSSION

The majority of ocular *C. trachomatis* infections occur in children, who have the highest loads and most severe active trachoma. However, infection predominantly occurs at low bacterial loads in the population overall. Similar findings have been observed in other studies [17,20,22], though we found a greater prevalence of infection across all age groups typical of hyperendemic settings. Almost half the individuals with quantifiable infection had a normal clinical phenotype, though the mean *C. trachomatis* load was significantly lower than in those with active trachoma, which is consistent with other studies in meso and hyperendemic settings [22,37].

In this population *C. trachomatis* load increases with disease severity (for both follicular (F) and inflammatory (P) scores), the strongest association being with increasing P-scores. The

association between ocular *C. trachomatis* load and disease severity in trachoma is supported by findings from other studies [16,17,22,38]. The association between *C. trachomatis* load and high F-scores is in part due to collinearity between F and P, where with high F-scores there is likely to be inflammation present. Inflammation has previously been found to be associated with high *C. trachomatis* loads and persistence of infection in children [39]. This is consistent with the high prevalence of infection and the spectrum of load and phenotype observed in this age group but may also be associated with pathogen virulence if there are different *C. trachomatis* strains in circulation. Further analysis is underway to investigate associations between pathogen genotype, clinical phenotype and geospatial clustering of strains.

There is spatial dependence in the distribution of *C. trachomatis* infection, demonstrated by positive spatial autocorrelation. The distance over which this occurs (1719m) equates to that of village boundaries. We used this data-driven threshold in our geostatistical models to account for the difficulties in performing this type of analysis in small island populations.

Our data show that the highest burden of infection (and load) is in children under ten years of age. There are usually only one or two children of this age group within a household in these communities [11]. The high load clusters (HH) and high load outliers (HL) are geographically close to the non-significant clusters and both exist within the village boundaries in this study (less than 200m apart). These data support the hypothesis that transmission occurs at village level in this population. Spread from an individual within an HH cluster to an individual in a non-significant cluster is also possible and requires further investigation in longitudinal and mathematical modelling studies.

Although household and village-level clustering is evident in active trachoma and ocular *C. trachomatis* infection [11,40-42], the inclusion of this spatial structure in regression models for active trachoma and *C. trachomatis* infection further improves model fit and demonstrates underlying spatial processes in the relationship between infection and disease, such that cases of active trachoma may represent recent exposure to *C. trachomatis* infection. The effect of spatial dependence in infection is greater than in active trachoma, perhaps reflecting the complexity of the disease process, where host-pathogen interactions contribute.

There was no global spatial autocorrelation evident for *C. trachomatis* bacterial load, likely reflecting the stronger influence of underlying social and biological rather than spatial processes. However, we were able to use local indicators of spatial association to examine fine-scale spatial clustering to identify clustering of high load infections. Spatial clusters, independent of age and gender, of individual infections with high bacterial loads (HH) and high load outliers that cluster with other low loads (HL) exist. Furthermore, there was no evidence of clustering of low load infections (LL), suggesting that high load infections may be important in transmission of chlamydial infection. There appears to be a threshold of *C. trachomatis* load below which HH clustering (and being a HL outlier) does not occur. The same phenomena were observed in data including infected and uninfected individuals and data with infected individuals only suggesting that low load infection may represent a negligible risk of transmission. This supports the described Allee effect, which hypothesizes that a reduction in chlamydial fitness due to reduced pathogen population size or density results in its disappearance from a population [43].

There are a limited number of studies that have assessed the spatial distribution of trachoma [5,7,44] and ocular *C. trachomatis* infection [45,46]. Broman *et al.* did not find clustering of active trachoma in children under the age of 10 years, but found clusters of households with high bacterial loads (defined as the household mean load) in treatment-naïve communities, supporting the findings in this study [45]. Yohannan *et al*. examined binary household-level data using a K-function nearest neighbours analysis [46]. The methodology for cluster detection in these studies was heterogeneous and measures of spatial dependence were not included in these analyses.

This cross-sectional study is limited in the assumption of load and clinical disease severity as a steady state. There are few data addressing stability of *C. trachomatis* load and disease phenotype (39). Bobo *et al.* conducted weekly surveys for three months in hyperendemic communities, finding that 62% of children had at least one infection during that time and of those 64% were persistently infected and had higher mean *C. trachomatis* loads and more severe disease than those who were sporadically infected [39]. Additionally, host conjunctival immune response and duration of infection add complexity to the interaction between *C. trachomatis* infection and disease severity [20,47]. *C. trachomatis* strain diversity may also be associated

with bacterial load, the spectrum of disease severity and the clustering of high load infections within these communities.

The role and importance of HH clusters and HL outliers in *C. trachomatis* transmission is speculative, but their presence, and the absence of low load clusters (LL) and low load outliers (LH), suggest that *C. trachomatis* load may have a role in transmission, and that these clusters may represent a source for spread of ocular *C. trachomatis* infection. Studies in trachoma and *C. trachomatis* infection in mouse models have suggested that *C. trachomatis* load is associated with transmission [37,48]. There is also some evidence from studies of urogenital *C. trachomatis* infection in humans that individuals with asymptomatic infection have lower *C. trachomatis* loads than individuals with symptomatic infections [49] and that the chance of sexual transmission of *C. trachomatis* per sexual act may be influenced by load [50]. However, the determinants of *C. trachomatis* load and its role in transmission and the development of sequelae are not well understood [51]. Further longitudinal data in the context of trachoma endemicity and mass drug treatment are required to fully address these questions and investigate the dynamics of *C. trachomatis* load in transmission.

Conclusion

This is the first study to use individual-level quantifiable *C. trachomatis* infections from a geospatially representative population-based sample to investigate spatial clustering of *C. trachomatis* infection. These data show that increasing *C. trachomatis* load is related to increasing disease severity in active trachoma, particularly with respect to inflammation. We have provided a global statistical measure for spatial autocorrelation in infection and disease and used local indicators of spatial association to describe the location and nature of the clusters in relation to *C. trachomatis* load.

These data suggest that high load *C. trachomatis* infections cluster spatially and may be important in transmission, although further longitudinal study is required. Further epidemiological and *in vitro* studies are required to provide a more complete picture of the relationship between disease severity and chlamydial load.

These geospatial tools may be useful as tools in trachoma surveillance to identify clusters of infection and thresholds of *C. trachomatis* bacterial load that may be important foci of transmission. Using these methods in conjunction with novel molecular tools to better define *C.*

trachomatis strains and ‘virulence’ may also improve our understanding of *C. trachomatis* pathogenesis and transmission.

Funding

This work was supported by a Wellcome Trust Clinical Research Training Fellowship (grant number 097330/Z/11/Z).

Acknowledgements

We extend thanks to colleagues in the Programa Nacional de Saúde de Visão in Bissau and to the communities of the Bijagós Archipelago, our field research team and all study participants in Guinea Bissau.

References

[1] Dawson CR, Jones BR, Tarizzo ML (1981). Guide to trachoma control in programs for the prevention of blindness; Geneva: World Health Organization.

[2] Thylefors B, Dawson CR, Jones BR, West SK, Taylor HR (1987). A simple system for the assessment of trachoma and its complicatios. Bull World Health Organ 65(4):477-83.

[3] Kuper H, Solomon AW, Buchan J, Zondervan M, Foster A, Mabey D (2003). A critical review of the SAFE strategy for the prevention of blinding trachoma. Lancet Infect Dis 3:372-381.

[4] Smith JL, Sturrock HJ, Olives C, Solomon AW, Brooker SJ (2013). Comparing the performance of cluster random sampling and integrated threshold mapping for targeting trachoma control, using computer simulation. PLoS Negl Trop Dis 7(8):e2389.

[5] Smith JL, Flueckiger RL, Hooper PJ, Polack S, Cromwell EA et al (2013). The geographical distribution and burden of trachoma in Africa. PLoS Negl Trop Dis 7(8):e2359.

[6] Smith JL, Haddad D, Polack S, Harding-Esch EM, Hooper PJ et al (2011). Mapping the global distribution of trachoma: why an updated atlas is needed. PLoS Negl Trop Dis 5(6):e973.

[7] Clements AC, Kur LW, Gatpan G, Ngondi JM, Emerson PM et al (2010). Targeting trachoma control through risk mapping: the example of Southern Sudan. PLoS Negl Trop Dis 4(8):e799.

[8] Baker MC, Mathieu E, Fleming FM, Deming M, King JD et al (2010). Mapping, monitoring and surveillance of neglected tropical diseases: towards a framework. Lancet 375(9710):231-8.

[9] Van der Linde HA, Dankin MH (1998). Enhancing Sustainability: Resources for our future. SUI Technical Series Volume 1. Proceedings of a workshop held at the world conservation congress for the Sustainable Use Initiative (SUI). IUCN, The World Conservation Union, Montreal Canada.

[10] World Bank. From the Climatic Research Unit (CRU) at the University of East Anglia (UEA) (2013). Climate Change Knowledge Portal: Guinea Bissau.

(http://sdwebx.worldbank.org/climateportal/index.cfm?page=country_historical_climate&ThisRegion=Africa&ThisCCode=GNB).

[11] Last AR, Burr SE, Weiss HA, Harding-Esch EM, Cassama E et al (2014). Risk Factors for Active Trachoma and Ocular *Chlamydia trachomatis* Infection in Treatment-naïve Trachoma-hyperendemic Communities of the Bijagós Archipelago, Guinea Bissau. PLoS Negl Trop Dis 8(6):e2900.

[12] Roberts CH, Last A, Molina-Gonzalez S, Cassama E, Butcher R et al (2013). Development and evaluation of a next generation digital PCR diagnostic assay for ocular *Chlamydia trachomatis* infections. J Clin Microbiol 51(7):2195-2203.

[13] Last A, Roberts CH, Cassama E, Nabicassa M, Molina-Gonzalez S et al (2014). Plasmid copy number and disease severity in naturally occurring ocular *Chlamydia trachomatis* infection. J Clin Microbiol 52(1):324-7.

[14] Harding-Esch E, Edwards T, Mkocha H, Munoz B, Holland MJ et al (2010). Trachoma prevalence and associated risk factors in The Gambia and Tanzania: Baseline results of a cluster randomized controlled trial. PLoS Negl Trop Dis 4(11):e861.

[15] Edwards T, Harding-Esch EM, Hailu G, Andreason A, Mabey DC et al (2008). Risk factors for active trachoma and *Chlamydia trachomatis* infection in rural Ethiopia after mass treatment with azithromycin. Trop Med Int Health 13:556-565.

[16] Burton MJ, Holland MJ, Faal N, Aryee EA, Alexander ND et al (2003). Which members of a community need antibiotics to control trachoma? Conjunctival *Chlamydia trachomatis* infection load in Gambian villages. Invest Ophthalmol Vis Sci 10(42):4215-22.

[17] Burton MJ, Holland MJ, Jeffries D, Mabey DC, Bailey RL (2006). Conjunctival Chlamydial 16S Ribosomal RNA Expression in Trachoma: Is Chlamydial Metabolic Activity Required for Disease to Develop? Clin Infect Dis 42:463-70.

[18] Keenan JD, Lakew T, Alemayehu W, Melese M, Porco TC et al (2010). Clinical activity and polymerase chain reaction evidence of chlamydial infection after repeated mass antibiotic treatments for trachoma. Am J Trop Med Hyg 82(3):482-7.

[19] Stare D, Harding-Esch E, Munoz B, Bailey R, Mabey D et al (2011). Design and baseline data of a randomised trial to evaluate coverage and frequency of mass

treatment with azithromycin: The Partnership for the Rapid Elimination of Trachoma (PRET) in Tanzania and The Gambia. Ophthalmic Epidemiol 18(1):20-9.

[20] Faal N, Bailey RL, Jeffries D, Joof H, Sarr I et al (2006). Conjunctival FOXP3 expression in trachoma: Do regulatory T cells have a role in human ocular *Chlamydia trachomatis* infection? PLoS Med 3(8):e266.

[21] West SK, Moncada J, Munoz B, Mkocha H, Storey et al. (2014). Is there evidence for resistance of ocular *Chlamydia trachomatis* to azithromycin after mass treatment for trachoma control? J Infect Dis 210(1):65-71.

[22] Solomon AW, Holland MJ, Burton MJ, West SK, Alexander ND et al (2003). Strategies for control of trachoma: observational study with quantitative PCR. Lancet 362(9379):198-204.

[23] Andreasen AA, Burton MJ, Holland MJ, Polley S, Faal N et al. (2008). *Chlamydia trachomatis ompA* variants in trachoma: what do they tell us? PLoS Negl Trop Dis 2(9):e306.

[24] Solomon AW, Holland MJ, Alexander ND, Massae PA, Aguirre A et al. (2004). Mass Treatment with Single-Dose Azithromycin for Trachoma. N Engl J Med 351:1962-1971.

[25] Alexander ND, Solomon AW, Holland MJ, Bailey RL, West SK et al. (2005). An index of community ocular *Chlamydia trachomatis* load for control of trachoma. Trans R Soc Trop Med Hyg 99(3):175-77.

[26] Jalal H, Verlander NQ, Kumar N, Bentley N, Carne C, Sonnex C (2011). Genital Chlamydial infection: association between clinical features, organism genotype and load. J Med Microbiol 60:881-8.

[27] Ruxton GD, Beauchamp G (2008). Time for some a priori thinking about post hoc testing. Behav Ecol 19(3):690-3.

[28] Bivand R (2010). Spdep: Spatial dependence: Weighting schemes, statistics and models. R package version 0.5-4. (http://CRAN.Rproject.org/package=spdep).

[29] Hiemstra PH, Pebesma EJ, Twenhofel CJW, Heuvelink GBM (2009). Real-time automatic interpolation of ambient gamma dose rates from the Dutch Radioactivity Monitoring Network. Computers & Geosciences 35(8):1711-1721.

[30] Pinheiro J, Bates D, DebRoy S, Sarkar D and R Core Team (2014). nlme: Linear and Nonlinear Mixed Effects Models. R package version 3.1-117 (http://CRAN.R-project.org/package=nlme).

[31] Chang K (2010). An introduction to geographic information systems (5th edition). New York:Thomas D. Timp pp327-40.

[32] Moran PA (1950). Notes on continuous stochastic phenomena. Biometrika 37(1-2):17-23.

[33] Cliff AD, Ord JK (1981). Spatial Processes. Pion pp63-5.

[34] Diggle PJ, Tawn JA, Moyeed RA (1998). Model-based geostatistics. Royal Statistics Society. Applied Statistics 47(3):299-350.

[35] Zucchini W (2000). An Introduction to Model Selection. J Mathematical Psychol 44:41-61.

[36] Anselin L (1995). Local indicators of spatial Association: LISA. Geographical Analysis 27(2):93-115.

[37] West ES, Munoz B, Mkocha H, Holland MJ, Aguirre A et al (2005). Mass treatment and the effect of the load in *Chlamydia trachomatis* infection in a trachoma-hyperendemic community. Invest Ophthalmol Vis Sci 46(1):83-7.

[38] Michel CE, Roper G, Devina MA, Lee HH, Taylor HR (2011). Correlation of clinical trachoma and infection in Aboriginal communities. PLoS Negl Trop Dis 5(3):e986.

[39] Bobo LD, Novak M, Munoz B, Hsieh YH, Quinn TC, West SK (1997). Severe disease in children with trachoma is associated with persistent *Chlamydia trachomatis* infection. J Infect Dis 176:1524-30.

[40] Bailey R, Osmond C, Mabey DC, Whittle HC, Ward ME (1989). Analysis of the household distribution of trachoma in a Gambian village using a Monte Carlo simulation procedure. Int J Epiemiol 18(4):944-51.

[41] Blake IM, Burton MJ, Bailey RL, Solomon AW, West S (2009). Estimating household and community transmission of ocular *Chlamydia trachomatis*. PLoS Negl Trop Dis 3(3):e401.

[42] Hagi M, Schemann JF, Mauny F, Momo G, Sacko D et al (2010). Active trachoma among children in Mali: Clustering and environmental risk factors. PLoS Negl Trop Dis 4(1):e583.

[43] Chidambaram JD, Lee DC, Porco TC, Lietman TM (2005). Mass antibiotics for trachoma and the Allee effect. Lancet Inf Dis 5(4):194-6.

[44] Polack SR, Solomon AW, Alexander NDE, Massae PA, Safari S et al (2005). The household distribution of trachoma in a Tanzanian village: an application of GIS to the study of trachoma. Trans Royal Soc Med Hyg 99:218-25.

[45] Broman AT, Shum K, Munoz B, Duncan DD, West SK (2006). Spatial clustering of ocular chlamydial infection over time following treatment, among households in a village in Tanzania. Invest Ophth Vis Sci 47(1):99-104.

[46] Yohannan J, He B, Wang J, Greene G, Schein Y et al (2014). Geospatial distribution and clustering of *Chlamydia trachomatis* in communities undergoing mass azithromycin treatment. Int Ophth Vis Sci 55(7):4144-50.

[47] Gambhir M, Basanez MG, Burton MJ, Solomon AW, Bailey RL et al (2009). The development of an age structured model for trachoma transmission dynamics, pathogenesis and control. PLoS Negl Trop Dis 3(6):e46.

[48] Pal S, Hui W, Peterson EM, de la Maza LM (1998). Factors influencing the induction of infertility in a mouse model of *Chlamydia trachomatis* ascending genital tract infection. J Med Microbiol 47(7):599-605.

[49] Wiggins R, Graf S, Low N, Horner PJ (Group CSSS) (2009). Real-time quantitative PCR to determine Chlamydial load in men and women in a community setting. J Clin Microbiol 47(6):1824-9.

[50] Dirks JAMC, Wolffs PFG, Dukers-Muijrers NHTM, Brink AATP, Speksnijder AGCL, Hoebe CJPA (2015). *Chlamydia trachomatis* load in population-based screening and STI clinics: Implications for screening policy. PLoS ONE 10(3):e0121433.

[51] Vodstrcil LA, McIver R, Huston WM, Tabrizi SN, Timms P, Hocking JS (2014). The epidemiology of organism load in genital *Chlamydia trachomatis* infection – a systematic review. J Inf Dis 211(10):1628-1645.

Figure 1. The Bijagós Archipelago, Guinea Bissau

Figure 1. The Bijagós Archipelago, Guinea Bissau (© Ezilon 2009). The islands of Bubaque, Canhabaque, Rubane and Soga (circled in red) were included in the current study.

Figure 2. *Chlamydia trachomatis* load by age and clinical phenotype in infected individuals

y-axis shows the natural logarithmic scale of *C. trachomatis* bacterial load (*omcB* copies/swab)

Figure 2. *Chlamydia trachomatis* load by age and clinical phenotype in infected individuals. The y axis shows the natural logarithmic scale of *C. trachomatis* bacterial load (*omcB* copies/swab).

Figure 3. Empirical semivariograms and fitted models for household prevalence of (a) ocular *Chlamydia trachomatis* infection and (b) active trachoma and the distribution of (c) ocular *Chlamydia trachomatis* bacterial load

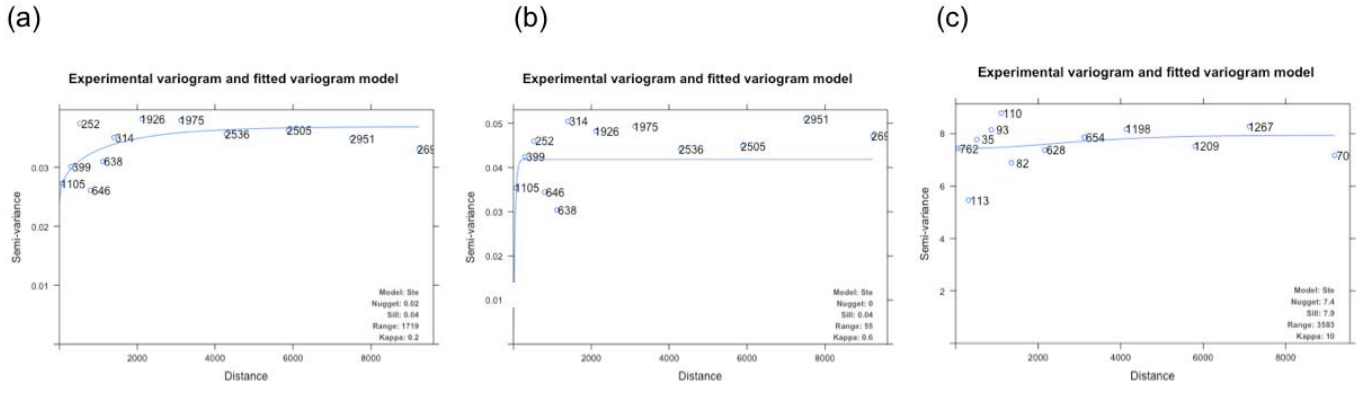

(a) Unadjusted household prevalence of *C. trachomatis* infection
(b) Household prevalence of active trachoma in 1-9 year olds
(c) Ocular *C. trachomatis* bacterial load

Prevalence data were log transformed (ln(ln+1)) due to significant negative skew. Active trachoma is defined as TF/TI by the WHO simplified grading system (2) (F2/3 or P3 by the modified FPC grading system (1)). Distance is indicated in (2) metres. Model fit with the smallest residual sum of squares (Matern, M.Stein's parameterization (Ste)). All values of Kappa (smoothing parameter of the Matern model) tested. Nugget, sill, range and Kappa are all estimated from the data.

Figure 3. Empirical semivariograms and fitted models for household prevalence of (a) ocular *C. trachomatis* infection (b) active trachoma and the distribution of (c) ocular *C. trachomatis* bacterial load.

(a) Unadjusted household prevalence of *C. trachomatis* infection
(b) Household prevalence of active trachoma in 1-9 year olds
(c) Ocular *C. trachomatis* bacterial load

Prevalence data were log transformed (ln(ln+1)) due to significant negative skew. Active trachoma is defined by TF/TI by the WHO Simplified Grading System [2] (F2/F3 or P3 by the Modified FPC Grading System [1]). Distance is indicated in metres. Model fit with the smallest residual sum of squares (Matern, M. Stein's Parameterization (Ste)). All values of Kappa (smoothing parameter of the Matern model) tested. Nugget, sill, range and Kappa are all estimated from the data.

C. trachomatis load was log transformed (ln(ln+1)) due to significant negative skew. Statistically significant positive values for the Local Moran's I statistic indicate clustering with similarly high (H-H) or low (L-L) values. Negative values indicate that neighbouring observations have dissimilar values and that this observation is an outlier (H-L or L-H). H-H clusters and H-L outliers are observed. There are no L-L clusters. Observation values represent *C. trachomatis* load. Adjacency is defined by the zone of indifference.

Figure 4. Clusters and outliers of high load ocular *Chlamydia trachomatis* infections. *C trachomatis* load log transformed (ln(ln+1)) due to significant negative skew. Statistically significant positive values for the Local Moran's I statistic indicate clustering with similarly high (H-H) or low (L-L) values. Negative values indicate that neighbouring observations have dissimilar values and that this observation is an outlier (H-L or L-H). H-H clusters and H-L outliers are observed. There are no L-L clusters. Observation values represent *C. trachomatis* load. Adjacency is defined by the zone of indifference.

Table 1. Estimated *Chlamydia trachomatis* load (*omcB* copies/swab) and analysis of variance (ANOVA[a]) by detailed clinical phenotype in infected individuals

Clinical Phenotype	*n*[b]	*omcB* copies/swab (Geometric Mean)	95% C.I. (SE geometric mean)	*p-Value* (ANOVA)			Median	Min	Max
Normal (F0P0C0)	71	294	165, 524	*Baseline*			176	15	96333
Active Trachoma (TF and/or TI)	92	8562	5412, 13546	***p<0.00001***			14236	17	274835
Scarring Trachoma (TS)	19	928	280, 3074	*p=0.4069*			2142	17	49125
Follicular Score (F)									
0	91	438	251, 762	*Baseline*			227	15	202632
1	20	1288	448, 3697	*p=0.324*	*Baseline*		1710	34	96333
2	27	3212	1264, 8165	***p=0.002***	*p=0.624*	*Baseline*	3203	27	140693
3	46	19870	2832, 25927	***p<0.0001***	***p<0.0001***	***p=0.018***	22767	323	274835
Inflammatory Score (P)									
0	46	122	68, 218	*Baseline*			67	15	41059
1	70	1534	871, 2702	***p<0.0001***	*Baseline*		1469	16	202632
2	46	10413	5461, 19857	***p<0.0001***	***p<0.0001***	*Baseline*	18569	17	274835
3	22	14053	5550, 35581	***p<0.0001***	***p<0.0001***	*p=0.964*	21864	34	158548
Scarring Score (C)									
0	155	1902	1207, 2996	*Baseline*			2095	15	274835
1	11	449	111, 1816	*p=0.438*	*Baseline*		204	34	11556
2	9	990	192, 5111	*p=0.927*	*p=0.941*	*Baseline*	589	76	54651
3	9	2475	253, 24192	*p=0.995*	*p=0.608*	*p=0.923*	7023	17	49125

[a]Scheffé correction used for multiple comparisons [b]*n*=number of individuals with quantifiable *C. trachomatis* bacterial load

Table 2. Multivariable mixed effects logistic regression analysis showing the effect of spatial dependence on clinically active trachoma and ocular *Chlamydia trachomatis* infection

Model	Predictor Variables	*n*	*AIC*[a]
C. trachomatis infection			
No spatial[b] *Spatial*[c]	age	1426	854.8 **801.8**
No spatial *Spatial*	age active trachoma[d]	1426 163	546.4 **495.6**
Active trachoma			
No Spatial *Spatial*	age	1426	697.9 **659.0**
No Spatial *Spatial*	age *C. trachomatis* infection	1426 224	389.5 **362.3**
No Spatial *Spatial*	age *C. trachomatis* load[e]	1426 180	251.2 **232.7**

[a]AIC=Akaike information criterion [b]With household or village as cluster variables [c]Including of spatial structure [d]defined as TF/TI using the WHO simplified grading system (2) [e]defined as log-(e) *omcB* copies/swab.

Table 3. Multivariable mixed effects linear regression analysis of factors predictive of *Chlamydia trachomatis* load (*omcB* copies/swab) in infected individuals

Model	Variable	*n*	OR[a]	95% C.I.	*p-Value*	*AIC*[b]	*BIC*[c]	*loglik*[d]
Null[e]								
						884.8	894.3	-439.4
Clustering								
Household[f]						884.3	893.8	-439.1
Village[f]						882.1	892.0	-438.2
Spatial[g]						799.7	834.8	-388.8
Final[h] *Including age and disease severity*								
Spatial						802.6	844.1	-388.3
No spatial						**797.7**	**829.6**	**-388.8**
Age	0-5 years	87	2.60	0.99, 6.87	**0.052**			
	6-10 years	45	0.70	0.24, 2.05	0.509			
	11-15 years	15	1.77	0.43, 7.20	0.427			
	>15 years	37	1.00	--	--			
Disease Severity	Inflammatory Grade (P)							
	0	46	1.00	--	--			
	1	70	7.54	3.12, 18.20	**<0.0001**			
	2	46	22.8	8.15, 63.9	**<0.0001**			
	3	22	30.9	9.39, 101.50	**<0.0001**			
	Follicular Grade (F)							
	0	91	1.00	--	--			
	1	20	1.29	0.43, 3.84	0.649			
	2	27	2.20	0.82, 5.88	0.114			
	3	46	7.78	3.16, 19.15	**<0.0001**			

C. trachomatis load is defined as log-(e) *omcB* copies/swab. There was no evidence of heteroscedasticity of residuals (Breusch-Pagan/Cook Weisberg test for heteroscedasticity in the final model. (Chi2 = 0.44, *p=0.5079*)) [a]Exponentiated coefficient [b]AIC=Akaike information criterion [c]BIC=Bayesian information criterion [d]loglik=Log likelihoood [e]Null model with dummy cluster variable [f]Including household or village as cluster variables on outcome [g]Including spatial structure [h]Final model including covariates with and without adjustment for spatial structure